Gao et al. EURASIP Journal on Wireless Communications and Networking 2011, 2011:99
http://jwcn.eurasipjournals.com/content/2011/1/99

EURASIP Journal on
Wireless Communications and Networking
a SpringerOpen Journal

RESEARCH Open Access

Hop-distance relationship analysis with quasi-UDG model for node localization in wireless sensor networks

Deyun Gao[1], Ping Chen[2], Chuan Heng Foh[3*] and Yanchao Niu[1]

Abstract

In wireless sensor networks (WSNs), location information plays an important role in many fundamental services which includes geographic routing, target tracking, location-based coverage, topology control, and others. One promising approach in sensor network localization is the determination of location based on hop counts. A critical priori of this approach that directly influences the accuracy of location estimation is the hop-distance relationship. However, most of the related works on the hop-distance relationship assume the unit-disk graph (UDG) model that is unrealistic in a practical scenario. In this paper, we formulate the hop-distance relationship for quasi-UDG model in WSNs where sensor nodes are randomly and independently deployed in a circular region based on a Poisson point process. Different from the UDG model, quasi-UDG model has the non-uniformity property for connectivity. We derive an approximated recursive expression for the probability of the hop count with a given geographic distance. The border effect and dependence problem are also taken into consideration. Furthermore, we give the expressions describing the distribution of distance with known hop counts for inner nodes and those suffered from the border effect where we discover the insignificance of the border effect. The analytical results are validated by simulations showing the accuracy of the employed approximation. Besides, we demonstrate the localization application of the formulated relationship and show the accuracy improvement in the WSN localization.

1 Introduction

In recent years, wireless sensor networks (WSNs) which generally consist of a large number of small, inexpensive and energy efficient sensor nodes have become one of the most important and basic technologies for information access [1]. WSNs have been widely used in military, environment monitoring, medicine care, and transportation control. Spatial information is crucial for sensor data to be interpreted meaningfully in many domains such as environmental monitoring, smart building failure detection, and military target tracking. The location information of sensors also helps facilitate WSN operation such as routing to a geographic field of interests, measuring quality of coverage, and achieving traffic load balance. In many monitoring applications, the sensor nodes must be aware its location to explain 'what happens and where'.

While specialized localization devices exist such as GPS, given the large number of sensor nodes involved in building a single WSN, it is cost ineffective to equip every sensor node with such a sophisticated device. Therefore, seeking for an alternative localization technology in WSNs has become one major research in WSNs [2]. Over the past few years, many localization algorithms have been proposed to provide sensor localization [3]. These localization protocols can be divided into two categories: range-based and range-free. The former is defined by methods that use absolute point-to-point distance estimates (range) or angle estimates for computing locations. The latter makes no assumption about the availability or validity of such information. Recently, range-free localization methods have attracted much attention because no extra sophisticated device for distance measurement is needed for each sensor node. Despite the challenge in obtaining virtual

* Correspondence: aschfoh@ntu.edu.sg
[3]School of Computer Engineering, Nanyang Technological University, 639798, Singapore
Full list of author information is available at the end of the article

coordinates purely based on radio connectivity information [4,5], attempts have been made in developing a practical solution to achieve localization. A few representative protocols of this range-free scheme include DV-Hop [6], APIT [7], DRLS [8], MDS-MAP [9], and LS-SOM [10]. Most of the range-free localization schemes, such as DV-Hop, need to compute the average distance per hop to estimate a node's location. In other words, the performance of these localization schemes relies on the accuracy of the employed hop-distance relationship. Since the determination of an accurate hop-distance relationship depends on various complex factors such as node deployment, node density, and wireless communication technology that cannot be easily quantified, the deduction process is tedious and unlikely to produce an exact close form relationship using, say the geometric methods [11].

Due to lack of any predetermined infrastructure and self-organized nature, in most cases, the sensor nodes are randomly and independently deployed in a bounded area. For simplicity, the vast majority of studies based on the idealized unit-disk graph (UDG) network model, where any two sensors can directly communicate with each other if and only if their geographic distance is smaller than a predetermined radio range. Examples of these research include geo-routing protocols [12,13], localization algorithms [8,14], and topology control techniques [15,16]. Similarly, most of the works related to the hop-distance relationship have been investigated assuming the UDG model [11,17-23]. The probability that two randomly selected stations with a known distance can communicate in K or less hops with omnidirectional antennas has been analyzed by Chandler [17]. Bettestetter and Eberspacher, derived the probability of the distance of two randomly chosen nodes deployed in a rectangular region within one or two hops [18]. However, when the hop counts are larger than two, only simulation results are available. The distribution parameters are computed by the iterative formula which extends from [19] with a linear formation. Ekici et al. [20] studied the probability of the k-hop distance in two dimensional network based on the approximated Gaussian distribution. Dulman et al. [11] derived the relationship between the number of hops separating two nodes and the physical distance between them in one- and two-dimensional topologies considering the UDG model. In the study, the approximated approach based on a Markov Chain in two-dimensional case is rather complicated to compute. Zhao and Liang [21] collected the hop-distance joint distribution from Monte Carlo simulations in a circular region and proposed an attenuated Gaussian approximation for the conditional probability distribution function (pdf) of the Euclidean distance given a known hop count. Ta et al. [22] provided a recursive equation for the two randomly located sensor nodes that are k-hop neighbors given a known distance in homogeneous wireless sensor networks. Ma et al. [23] proposed a method to compute the conditional probability that a destination node has hop-count h with respect to a source node given that the distance between the source and the destination is d.

Despite the current efforts, no fixed communication range exists in actual network environment for the reasons such as multi-path fading and antenna issues. Therefore, a certain level of deviation occurs between the intended operation and actual operation in wireless sensor networks when the UDG model is assumed in a protocol design. To deal with this problem, a practical model called the quasi Unit-disk Graph (quasi-UDG) model is proposed recently [24]. The quasi-UDG model can be characterized by two parameters, the radio range R and the quasi-UDG factor α. For any two nodes in the quasi-UDG model, if their distance is longer than R, no direct communication link exists between the two. Otherwise, if their distance is between αR and R, a communication link exists with a probability of p_l, and p_l = 1 when their distance is shorter than αR. Given this newly proposed practical property of connectivity, it warrants an investigation of the hop-distance relationship with the quasi-UDG model for the range-free localization schemes to capture practical connectivity characteristics.

In this paper, we focus on exploiting the connectivity property of the quasi-UDG model and analyze the relationship between the hop counts separating two nodes and their geographic distance with a specific node density in a WSN. We seek approximation technique to provide a scalable solution for the two-dimensional case. We further demonstrate the application of the developed hop-distance relationship to a range-free localization scheme.

In our WSN setup, we consider that sensor nodes are deployed into a circular region S_b with the radius R_b, where the deployment position follows a Poisson point process with a certain density λ. We set $p_l = \frac{\alpha}{1-\alpha}\left(\frac{R}{d}-1\right)$ such that a longer distance between two nodes has a lower probability to form a direct communication link. With this setup, we formulate the probability that a pair of nodes with a known distance resulting a particular hop count. Additionally, we also develop the probability that a pair of nodes with a known distance gives a particular hop count. Finally, in our analysis, we present a quantitative evaluation for the border effect of geographic distance distribution with a given hop count.

The rest of this paper is organized as follows. In Section 2, we present our analytical model deriving an approximate recursive formula for the hop-distance relationship considering the quasi-UDG model. Section 3 extends our analytical model by taking the border effect and dependence problem into consideration. Section 4 formulates the probability distribution of distance with known hop counts. In Section 5, we demonstrate the use of our developed hop-distance relationship by applying the relationship to a least squares (LS) based localization algorithm. Finally, we report results in Section 6 and draw important conclusions in Section 7.

2 The probability of the hop count given a known distance

In general, the hop-distance relationship is influenced by the density of sensor nodes and their deployment strategy, as well as the radio communication characteristics. Considering the more practical quasi-UDG model, it is recognized that the formulation for the hop-distance relationship with the consideration of quasi-UDG model is tedious and unlikely to produce an exact close form. We seek approximation using a recursive approach to derive an approximated hop-distance relationship. In this section, we focus on analyzing the probability that a particular pair of sensor nodes forms a certain hop count with a known distance.

Suppose that N sensor nodes are deployed randomly in circular region S_b with a radius R_b. The number of nodes in any region is a Poisson random variable with an average node density of $\lambda = \frac{N}{S_b} = \frac{N}{(\pi R_b^2)}$. Assume that the communication range of a node is R, the communication model between any pair of nodes follows the quasi-UDG model with a factor of α where $0 < \alpha < 1$.

With the quasi-UDG model, the communication area between two nodes with the distance d can be further divided into three cases shown as follows.

- If $d \le \alpha R$, then the two nodes can communicate directly.
- If $\alpha R < d \le R$, then the two nodes can communicate with a probability p_l, which is set to $(R/d - 1)\alpha/(1 - \alpha)$. It means that a longer distance between two nodes has a lower probability to form a direct communication link.
- If $d > R$, then the two nodes cannot communicate directly.

The quasi-UDG model is illustrated with an example shown in Figure 1. In the figure, we assume that there are two nodes u and v, their distance is d_{uv}, and their communication probability is P. Let $\Phi_h(d)$ be the probability that a particular pair of nodes with d distance apart is h hops away from each other. In the following, we shall first derive $\Phi_h(d)$ for the case of $h = 1$ and then $h \ge 2$.

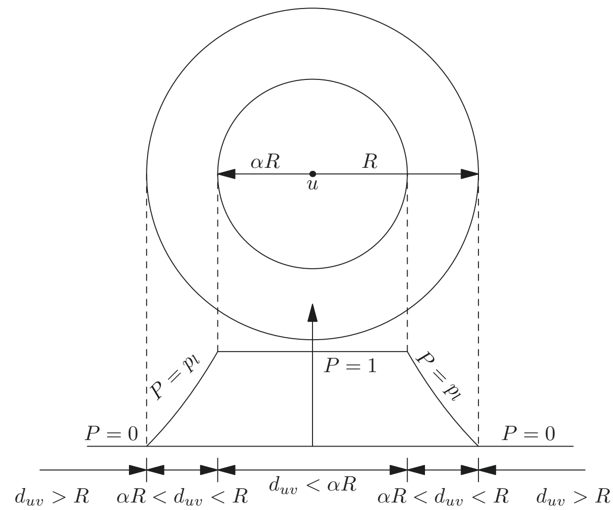

Figure 1 Quasi-UDG model.

2.1 The case of $h = 1$

For the case of $h = 1$, owing to the quasi-UDG model, $\Phi_1(d)$ is obviously

$$\Phi_1(d) = \begin{cases} 1 & d \le \alpha R \\ \frac{\alpha}{1-\alpha}\left(\frac{R}{d} - 1\right) & \alpha R < d \le R \\ 0 & d > R \end{cases} \tag{1}$$

2.2 The case of $h \ge 2$

We first note that two nodes, named O_1 and O_2, have no direct link but may communicate through h - 1 relay nodes. This gives rise to two possibilities, where

- O_2 is not the m-hop neighbor of O_1 if $m < h$.
- Within the communication range of O_2, there is a least one (h - 1)-hop neighbor of O_1 that has a direct link with O_2.

For $m < h$, the probability, P_N, that O_2 is not the m-hop neighbor of O_1 can be obtained as

$$P_N = 1 - \sum_{m=1}^{h-1} \Phi_m(d). \tag{2}$$

We shall now consider the second possibility in the following. Considering two circles which one centered at O_1 having a radius of r and the other centered at O_2 having a radius of R. We denote the distance between the two centers as d and refer the common region of the two circles as S. The quantity $P_r(S)$ is defined as the probability that in the area S, there is no (h - 1)-hop neighbor of O_1 that can communicate with O_2 directly. A differential increment of dr on r can obtain a differential incremental region of dS. Assume that the probability $\Phi_h(d)$ of any pair of nodes is independent and statistically identical, we

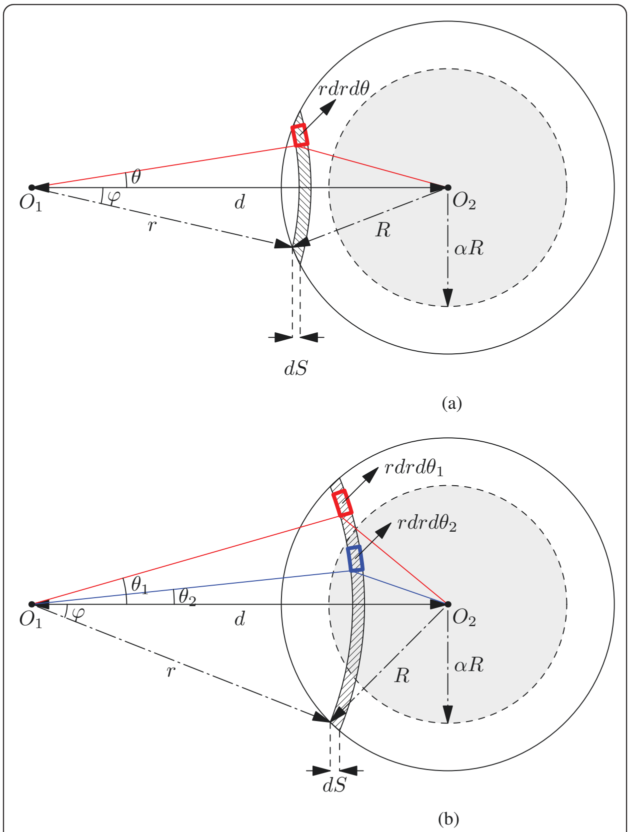

Figure 2 Illustration of ***dS*** **when** ***d*** **>** ***R*** **for the case that (a)** ***dS*** **locates in** $\mathcal{A}(O_2)$**, and (b)** ***dS*** **locates in** $\mathcal{C}(O_2)$ **and** $\mathcal{A}(O_2)$.

have $P_r(S+dS) = P_r(S)P_r(dS)$. In the following subsections, we calculate $P_r(dS)$ based on three conditions, which are $d > R$, $\frac{1+\alpha}{2}R < d < R$, and $\alpha R < d\frac{1+\alpha}{2}R$.

R",1,0,2,0,0pc,0pc,0pc,0pc>2.2.1 O_1 falls outside the communication range of O_2 where $d > R$

In Figure 2, we see that dS can be further divided into many differential regions $rdrd\theta$. Since dr and $d\theta$ are infinitesimal, the probability that there exists more than one sensor node in the region $rdrd\theta$ can be ignored, and the probability that a single sensor node located within $rdrd\theta$ can be approximated as $\lambda rdrd\theta$.

We term the circular region centered in O_2 with the radius αR as $\mathcal{C}(O_2)$, and the annulus region centered in O_2 with the larger radius R and the smaller one αR as $\mathcal{A}(O_2)$. There are two cases needed to be taken into consideration, which are

- When dS falls into $\mathcal{A}(O_2)$ as shown in Figure 2(a), r satisfies $d - R \le r \le d - \alpha R$ or $d + \alpha R \le r \le d - R$. With the definition of the quasi-UDG model, every differential region $rdrd\theta$ of dS has a corresponding probability p_l to communicate with O_2. Therefore, $P_r(dS)$ is given by (3) where

$$P_r(dS) = 1 - 2\Phi_{h-1}(r)\lambda rdr \int_0^{\varphi} \frac{\alpha}{1-\alpha}\left(\frac{R}{l}-1\right) d\theta. \quad (3)$$

As illustrated in Figure 2(a), we can get the following relationship

$$\varphi = \arccos \frac{r^2 + d^2 - R^2}{2rd} \quad (4)$$

$$l = \sqrt{r^2 + d^2 - 2rd\cos\theta}. \quad (5)$$

- When dS covers both $\mathcal{C}(O_2)$ and $\mathcal{A}(O_2)$, r will be bounded by $d - \alpha R \le r < d + \alpha R$. The part $rdrd\theta$ that falls within $\mathcal{C}(O_2)$ is surely a one-hop neighbor of O_2. When that part falls within $\mathcal{A}(O_2)$, it has a corresponding probability p_l that it has a direct link with O_2. Then $P_r(dS)$ can be determined by

$$P_r(dS) = 1 - 2\Phi_{h-1}(r)\lambda rdr \left[\varphi_1 + \int_{\varphi 1}^{\varphi} \frac{\alpha}{1-\alpha}\left(\frac{R}{l}-1\right) d\theta\right] \quad (6)$$

and

$$\varphi_1 = \arccos \frac{r^2 + d^2 - (\alpha R)^2}{2rd}. \quad (7)$$

2.2.2 O_1 falls within the communication range of O_1 and d satisfies $\frac{1+\alpha}{2}R < d < R$

We use the foregoing strategy for this derivation. We notice that there are three cases needed to be treated individually which are given as follows.

- If $0 < r < R - d$, dS will be the annulus region and the entire section of dS will fall within $\mathcal{A}(O_2)$, which gives

$$P_r(dS) = 1 - 2\Phi_{h-1}(r)\lambda rdr \int_0^{\pi} \frac{\alpha}{1-\alpha}\left(\frac{R}{l}-1\right) d\theta \quad (8)$$

- If $R\text{-}d \le r < d\text{-}\alpha R$ or $d+\alpha R \le r < R+d$, dS will not be the annulus region but the entire section of dS will still fall within $\mathcal{A}(O_2)$. Then we can obtain $P_r(dS)$ by (3).
- If $d\text{-}\alpha R \le r < d+\alpha R$, dS will cover both $\mathcal{C}(O_2)$ and $\mathcal{A}(O_2)$. In this case, we can determine $P_r(dS)$ by (6).

2.2.3 O_1 falls within the communication range of O_2 and d satisfies $\alpha R < d\frac{1+\alpha}{2}R$

There are four cases needed to be considered when O_1 falls within the communication range of O_2 and d

satisfying the condition $\alpha R < d\frac{1+\alpha}{2}R$, which are

- If $0 < r < d\text{-}\alpha R$, dS will be the annulus region and the entire section of dS will fall within $\mathcal{C}(O_2)$. Then we can determine $P_r(dS)$ by (8).
- If $d\text{-}\alpha R \le r < R\text{-}d$, dS will still be the annulus region but it covers both $\mathcal{C}(O_2)$ and $\mathcal{A}(O_2)$. Therefore, we have

$$P_r(dS) = 1 - 2\Phi_{h-1}(r)\lambda r\mathrm{d}r\left[\varphi_1 + \int\limits_{\varphi_1}^{\pi}\frac{\alpha}{1-\alpha}\left(\frac{R}{l}-1\right)\mathrm{d}\theta\right] \quad (9)$$

- If $R\text{-}d \le r < d+\alpha R$, dS will not be will the annulus region and it covers both $\mathcal{C}(O_2)$ and $\mathcal{A}(O_2)$. The probability $P_r(dS)$ can be obtained by (6).
- If $d+\alpha R \le r < R+d$, dS will fall within the region $\mathcal{A}(O_2)$, and hence we can compute $P_r(dS)$ by (3).

2.3 Determination of Φ_h (d) for $h \ge 2$

Consider that $P_r(dS)$ only depends on r with a specific d, we set $P_r(dS) = 1 - g(r)$. From $P_r(S + dS) = P_r(S)P_r(dS)$, the expression of $P_r(S)$ can be obtained by the following linear differential equation where

$$P_r(S) = \exp\left(-\int\limits_{d-R}^{d+R} g(r)\mathrm{d}r\right). \quad (10)$$

Therefore, with (2) and (10), the probability $\Phi_h(d)$ with $h \ge 2$ can be obtained as

$$\begin{aligned}\Phi_h(d) &= P_N \times (1 - P_r(S)) \\ &= \left(1 - \sum_{i=1}^{h-1}\Phi_i(d)\right)\left(1 - \exp\left(-2\lambda\Omega(\mathrm{d})\right)\right)\end{aligned} \quad (11)$$

where knowing d, $\Omega(d)$ can be determined by one of the following expressions, which are

- For $d > hR$ or $d < \alpha R$:

$$\Omega(d) = 0; \quad (12)$$

- For $R < d \le hR$:

$$\begin{aligned}\Omega(d) = &\int_{d-R}^{d-\alpha R}\Phi_{h-1}(r)r\int\limits_{0}^{\varphi}\frac{\alpha}{1-\alpha}\left(\frac{R}{l}-1\right)\mathrm{d}\theta\mathrm{d}r \\ &+ \int_{d-\alpha R}^{d+\alpha R}\Phi_{h-1}(r)r\left(\varphi_1 + \int\limits_{\varphi_1}^{\varphi}\frac{\alpha}{1-\alpha}\left(\frac{R}{l}-1\right)\mathrm{d}\theta\right)\mathrm{d}r \\ &+ \int_{d+\alpha R}^{d+R}\Phi_{h-1}(r)r\int\limits_{0}^{\varphi}\frac{\alpha}{1-\alpha}\left(\frac{R}{l}-1\right)\mathrm{d}\theta\mathrm{d}r\end{aligned} \quad (13)$$

- For $\frac{1+\alpha}{2}R < d \le R$:

$$\begin{aligned}\Omega(d) = &\int_{0}^{R-d}\Phi_{h-1}(r)r\int\limits_{0}^{\pi}\frac{\alpha}{1-\alpha}\left(\frac{R}{l}-1\right)\mathrm{d}\theta\mathrm{d}r \\ &+ \int_{R-d}^{d-\alpha R}\Phi_{h-1}(r)r\int\limits_{0}^{\varphi}\frac{\alpha}{1-\alpha}\left(\frac{R}{l}-1\right)\mathrm{d}\theta\mathrm{d}r \\ &+ \int_{d-\alpha R}^{d+\alpha R}\Phi_{h-1}(r)r(\varphi_1 + \int\limits_{\varphi_1}^{\varphi}\frac{\alpha}{1-\alpha}\left(\frac{R}{l}-1\right)\mathrm{d}\theta)\mathrm{d}r \\ &+ \int_{d+\alpha R}^{d+R}\Phi_{h-1}(r)r\int\limits_{0}^{\varphi}\frac{\alpha}{1-\alpha}\left(\frac{R}{l}-1\right)\mathrm{d}\theta\mathrm{d}r\end{aligned} \quad (14)$$

- For $\alpha R < d \le \frac{1+\alpha}{2}R$:

$$\begin{aligned}\Omega(d) = &\int_{0}^{d-\alpha R}\Phi_{h-1}(r)r\int\limits_{0}^{\pi}\frac{\alpha}{1-\alpha}\left(\frac{R}{l}-1\right)\mathrm{d}\theta\mathrm{d}r \\ &+ \int_{d-\alpha R}^{R-d}\Phi_{h-1}(r)r(\varphi_1 + \int\limits_{\varphi_1}^{\pi}\frac{\alpha}{1-\alpha}\left(\frac{R}{l}-1\right)\mathrm{d}\theta)\mathrm{d}r \\ &+ \int_{d-\alpha R}^{d+\alpha R}\Phi_{h-1}(r)r(\varphi_1 + \int\limits_{\varphi_1}^{\varphi}\frac{\alpha}{1-\alpha}\left(\frac{R}{l}-1\right)\mathrm{d}\theta)\mathrm{d}r \\ &+ \int_{d+\alpha R}^{d+R}\Phi_{h-1}(r)r\int\limits_{0}^{\varphi}\frac{\alpha}{1-\alpha}\left(\frac{R}{l}-1\right)\mathrm{d}\theta\mathrm{d}r.\end{aligned} \quad (15)$$

3 The border effect and dependence problem

In the above analysis, we do not consider borders of a WSN. However, in a realistic scenario, the deployment area of WSNs is finite and hence borders exist. It is known that the probability $\Phi_h(d)$ derived assuming that both involved nodes are not near the border of a WSN may give a slightly different result when one or both of them fall near the border. This is known as the border effect. One common handling of the border effect is to consider the toroidal distance metric in the simulation experiment where a node closed to the border can communicate directly with some nodes at the opposite border [25]. While this special setup eliminates the border effect, it creates discrepancy between the study and practical setups which may lead to a certain level of errors.

Clearly, nodes which are closer to the border cover smaller regions than those at least d away from the border, and therefore intuitively the quantity for $\Omega(d)$ should be smaller with the consideration of the border effect. Apparently, the border effect gives a different level of impacts in the measure of $\Phi_h(d)$ with a different distance between an involved node and the border.

However, it is tedious to derive all cases considering the border effect. For simplicity, we take two key cases of the border effect into consideration. Assuming the center of deployment area is O, we consider two annulus near the border in the following.

- The first annulus, called $\mathcal{A}_1(o)$, is between the circles with radius of R_b-R and R_b-αR.
- The second annulus, called $\mathcal{A}_2(o)$, is between the circles with radius of R_b-R and R_b-αR.

We set an average metric $\zeta(h)$ which varies from 0 to 1 for each hop to determine the decrement of $\Omega(d)$. For the circle area with the radius R_b - R, which can be called $\mathcal{C}(o)$, we can set $\zeta(h)$ = 1 accordingly.

Another factor we have to consider is the dependence. The hop-distance relationship derived as aforesaid relies on an implicit independence assumption, that is the probability $\Phi_h(d)$ of any pair of nodes is independent and statistically identical. However as pointed in [22], the events that those nodes with the direct link to O_2 are h - 1 hops away from O_1 are not mutually independent for cases when h >2, and the calculation of $\Phi_{h-1}(r)$ should include appropriate dependence conditions. For example, as shown in Figure 3, nodes O_1 and O_2 are d distance apart and h hops away from each other where h = 3. The probability that node M_1 is a 2-hop neighbor of node O_1 is the probability that there is at least one node located in the area S_1 offering packet relay between nodes O_1 and M_1. Here, the area S_1 is the intersect area between the circles with the centers O_1 and M_1. Similarly, the probability that node M_2 is a 2-hop neighbor of node O_1 is the probability that there is at least one node located in the area S_2 which can directly communicate with nodes O_1 and M_2. Here, the area S_2 is the intersect area between the circles with the centers O_1 and M_2. It is obvious in the figure that the areas S_1 and S_2 share a common area S_{12} indicating that the calculated probabilities are not independent.

To include the impact of the dependence, we add a new factor, namely $\xi(h)$, into the expression of $\Omega(d)$. Both factors $\zeta(h)$ and $\xi(h)$ are added to allow $\Omega(d)$ to reflect a practical setup, and they can be estimated by statistical results via experiments. With the inclusion of $\zeta(h)$ and $\xi(h)$ into the expression of $\omega(h)$, (11) becomes

$$\Phi_h(d) = \left(1 - \sum_{i=1}^{h-1} \Phi_i(d)\right)\left(1 - \exp\left(-2\lambda\omega(h)\Omega(d)\right)\right). \quad (16)$$

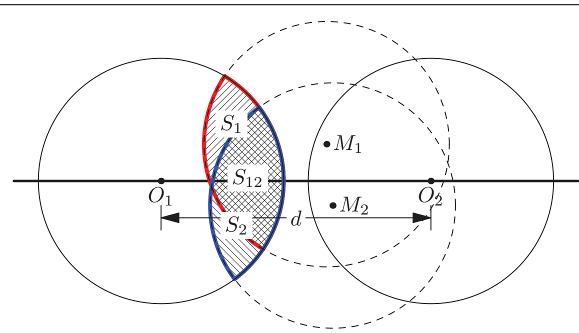

Figure 3 Illustration of multihop-dependence problem.

4 Distance distribution with known hop counts

In this section, assume that sensor nodes are randomly deployed in a circular region, we derive equations to determine the probability density function of distance d with a known hop count $f_{\mathcal{H}}(d)$.

Theorem 4.1 *The probability density function for the distance d between two nodes randomly deployed in a circular region with the radius R_b is $f_{\mathcal{D}}(d)$, where*

$$f_{\mathcal{D}}(d) = \frac{d}{\pi R_b^4}\left(4R_b^2 \arccos\left(\frac{d}{2R_b}\right) - d\sqrt{4R_b^2 - d^2}\right) \quad (17)$$

We provide the proof of Theorem 4.1 in Appendix A. According to Theorem 4.1, we can obtain the probability density function of distance between any two nodes in the areas $\mathcal{C}(o)$, $\mathcal{A}_1(o)$, and $\mathcal{A}_2(o)$. Their probability density functions of distance are $f_{\mathcal{D}_c}(d)$, $f_{\mathcal{D}_{\mathcal{A}_1}}(d)$, and $f_{\mathcal{D}_{\mathcal{A}_2}}(d)$, respectively. We also term them as $f_{\mathcal{D}*}(d)$, in general, where the symbol * is appropriately substituted by either $\mathcal{A}_1$, $\mathcal{A}_2$ or $\mathcal{C}$. Their expressions are given in (18), (19) and (20) in the following.

$$f_{\mathcal{D}_{\mathcal{A}_1}}(d) = \begin{cases} \frac{2d}{R_b^2} & 0 < d \le \alpha R \\ \frac{2d}{\pi R R_b^2(1-\alpha)(2R_b^2-\alpha R-R)}\left(\Lambda(R_b, R_b-\alpha R, d) - \pi(R_b-R)^2\right) & \alpha R < d \le R \\ \frac{2d}{\pi R R_b^2(1-\alpha)(2R_b^2-\alpha R-R)}\left(\Lambda(R_b, R_b-\alpha R, d) - \Lambda(R_b, R_b-R, d)\right) & R < d \le 2R_b - R \\ \frac{2d}{\pi R R_b^2(1-\alpha)(2R_b^2-\alpha R-R)}\Lambda(R_b, R_b-\alpha R, d) & 2R_b - R < d \le 2R_b - \alpha R \end{cases} \quad (18)$$

$$f_{\mathcal{D}_{\mathcal{A}_2}}(d) = \begin{cases} \frac{d}{\pi\alpha R R_b^2(2R_b-\alpha R)}\left(4R_b^2\arccos(\frac{d}{2R_b}) - d\sqrt{4R_b^2-d^2} - 2\pi(R_b-\alpha R)^2\right) & 0 < d \le \alpha R \\ \frac{d}{\pi\alpha R R_b^2(2R_b-\alpha R)}\left(4R_b^2\arccos(\frac{d}{2R_b}) - d\sqrt{4R_b^2-d^2} - 2\Lambda(R_b, R_b-\alpha R, d)\right) & \alpha R < d \le 2R_b - \alpha R \\ \frac{d}{\pi\alpha R R_b^2(2R_b-\alpha R)}\left(4R_b^2\arccos(\frac{d}{2R_b}) - d\sqrt{4R_b^2-d^2}\right) & 2R_b - \alpha R < d \le 2R_b \end{cases} \quad (19)$$

$$f_{\mathcal{D}_C}(d) = \frac{4d}{\pi(R_b-R)^2}\arccos\frac{d}{2(R_b-R)} - \frac{4d^2}{\pi(R_b-R)^4}\sqrt{4(R_b-R)^2-d^2} \quad s.\,t.\quad 0 < d \le 2\cdot(R_b-R) \quad (20)$$

where $\Lambda(R, r, d)$ is given by

$$\Lambda(R, r, d) = R^2\arccos\frac{R^2+d^2-r^2}{2dR} + r^2\arccos\frac{r^2+d^2-R^2}{2dr} - \frac{1}{2}\sqrt{((r+R)^2-d^2)(d^2-(R-r)^2)}.$$

By the Bayes' formula, given $f_{\mathcal{D}*}(d)$ and $\Phi_h(d)$, we can obtain the expression $f_{\mathcal{H}*}(d)$ which is the probability density function of the geographical distance d when the hop count h is known to be H^*. This expression is determined by

$$f_{\mathcal{H}*}(d) = \frac{\Phi_h(d) f_{\mathcal{D}*}(d)}{\int_{r_0}^{hR}\Phi_h(x) f_{\mathcal{D}*}(x)\,\mathrm{d}x} \quad (21)$$

where r_0 = 0 when h = 1, and r_0 = αR when h > 1.

5 Localization Applications

With the development of the hop-distance relationship for the quasi-UDG model, in this section, we show the application of this new relationship to a particular localization algorithm using LS based localization algorithms [26], and we call this newly designed localization algorithm enhance weighted least squares (EWLS).

In a particular localization scenario in WSNs, we assume that there is a number of nodes whose locations are known, and they shall be called anchor nodes. Other nodes that have no knowledge of their locations are called unknown nodes. Consider that an unknown node j can obtain the location $\mathbf{x}_i$, hop h_{ji} and average hop-distance c_i of an anchor node i. The distance between nodes j and i can be calculated as $d_{ji} = c_i h_{ji}$. In our test scenario, we place an anchor node o in the center and add several other anchor nodes in the map.

We design a simple mechanism to compute the range of distance d_{ji}. Each anchor node i collects some information to other anchor node k, computes and ranks the average hop-distance $c_{i(k)} = d_{ik}/h_{ik}$, such as $c_{i(1)} \geq c_{i(2)} \geq \ldots \geq c_{i(n)}$. We set the range of average hop-distance as

$$\underline{c}_i = \frac{\sum_{k=1}^{n-1} ||\mathbf{x}_i - \mathbf{x}_{(k)}\,||}{\sum_{k=1}^{n-1} h_{i(k)}} \leq c_i \leq \frac{\sum_{k=2}^{n} ||\mathbf{x}_i - \mathbf{x}_{(k)}\,||}{\sum_{k=2}^{n} h_{i(k)}} = \bar{c}_i \quad (22)$$

Following that, the range of distance d_{ji} can be computed as $d_{ji}^{(M)} = \bar{c}_i \times h_{ji}$ and $d_{ji}^{(m)} = \underline{c}_i \times h_{ji}$. With the range of distance d_{ji}, the variance v_h of the pdf $f_{\mathcal{H}}(d)$, we compute the weights, w_i, of measured distance d_{ji} as

$$w_i = \frac{1}{v_h \int_{d_{ji}^{(m)}}^{d_{ji}^{(M)}} f_{\mathcal{H}}(x)\mathrm{d}x}. \quad (23)$$

Finally, we set $W = \mathrm{diag}(w_1, \ldots, w_n)$ and compute the location $\hat{\mathbf{x}}$ of an unknown node using the following results, where

$$\hat{\mathbf{x}} = (A_n^T W A_n)^{-1} A_n^T W b_n \quad (24)$$

and

$$A_n = 2\begin{bmatrix} x_1 - \Omega(x_i) & y_1 - \Omega(y_i) \\ \vdots & \vdots \\ x_n - \Omega(x_i) & y_n - \Omega(y_i) \end{bmatrix}$$

$$b_n = \begin{bmatrix} x_1^2 - \Omega(x_i^2) + y_1^2 - \Omega(y_i^2) + \Omega(d_i^2) - d_1^2 \\ \vdots \\ x_n^2 - \Omega(x_i^2) + y_n^2 - \Omega(y_i^2) + \Omega(d_i^2) - d_n^2 \end{bmatrix}$$

$$\Omega(t) = \frac{\sum_{i=1}^{n} t w_i}{\sum_{i=1}^{n} w_i}.$$

6 Result discussions

In this section, we compare the analytical and statistical results through simulation experiments to illustrate the performance of our proposed hop-distance model. To illustrate the benefit of applying our model to LS-based localization algorithms, we compared our enhanced algorithm of EWLS to two classical LS-based localization algorithms namely LS [26] and PDM [27].

6.1 Impacts of boarder effects and dependence

We first illustrate the impacts of the boarder effect and dependence problem. In the experiments, we gather statistics of the hop counts with corresponding distance information using Monte Carlo simulations. All the simulation data are collected from several scenarios where N sensor nodes are randomly deployed in a circular region of radius R_b, and the transmission range is set to R with the consideration of the quasi-UDG model. The parameters are set to $N = 400$, $R_b = 200$, $R = 50$, $\alpha = 0.75$, and the result comparisons are listed in Table 1. Let o be the deployment center. The region where nodes are deployed away from the border is denoted as $\mathcal{C}(o)$, and we term $\mathcal{A}_1(o)$ and $\mathcal{A}_2(o)$ as the annulus regions in which the distances to o are within $(R_b\text{-}R, R_b\text{-}\alpha R]$ and $(R_b\text{-}\alpha R, R_b]$, respectively.

In Table 1 we use cumulative absolute difference (CAD) to measure the sum of absolute differences between the analytical results and statistical data. We set $CAD = \sum_d |\Phi_h(d) - Sim_h|$, where $\Phi_h(d)$ and Sim_h are the probabilities of two nodes giving a hop count of h with a known distance of d obtained from the analysis and simulation, respectively. Moreover, we denote CAD* as the CAD measurement between analytical results without the border effect consideration and statistical data. For $\mathcal{A}_1(o)$ and $\mathcal{A}_2(o)$, we can see that the CAD* of each hop is larger than that of CAD because of the impact of the border effect.

Table 1 Comparisons between analytical and simulation results of $\Phi_h(d)$

	Hops	2	3	4	5	6	7	8	9
$\mathcal{C}(o)$	CAD	0.34	0.36	0.85	1.49	2.12	2.76	3.36	3.9
	$\omega(h)$	1.0	0.77	0.70	0.65	0.63	0.60	0.58	0.54
$\mathcal{A}_1(o)$	CAD	0.42	0.38	0.86	1.52	2.13	2.69	3.31	3.98
	CAD*	0.66	0.59	0.88	1.59	2.21	2.79	3.45	4.03
	$\omega(h)$	0.95	0.77	0.70	0.65	0.62	0.61	0.59	0.57
$\mathcal{A}_2(o)$	CAD	0.35	0.49	1.17	1.76	2.33	2.89	3.40	4.05
	CAD*	0.74	0.75	1.19	1.85	2.45	3.06	3.61	4.16
	$\omega(h)$	0.92	0.77	0.69	0.65	0.62	0.61	0.59	0.58

6.2 The validation of distribution of distance by a known hop count

We conduct simulation experiments with N = 400, R_b = 200, R = 50, α = 0.75 and present $f_{\mathcal{H}*}(d)$ in Figures 4, 5 and 6 with the statistical data and our analytical results. In all three cases, we note that the numerical results of $f_{\mathcal{H}*}(d)$ given in (21) show excellent agreement with the simulation results. This excellent agreement confirms the accuracy of our model for the estimation of the distance given a known hop count between two sensor nodes.

6.3 Localization accuracy comparisons

In the following, we conduct several simulation experiments to illustrate the performance of our proposed EWLS algorithm. In the simulation, N = 100 sensor nodes are randomly deployed in the circle $\mathcal{S}_b$ with the radius R_b = 200. The number of anchor nodes is 16 and the communication range of each sensor node is R = 80. The factor α of the quasi-UDG model is set to 0.76. In Figure 7 (a), even within the communication range R of node 1, the nodes 30, 38, 53, and 63 cannot communicate directly with node 1 due to the considered quasi-UDG model. With the network topology illustrated in Figure 7(a), we show the localization errors of EWLS, LS, and PDM in Figure 7. Apparently, the accuracy of EWLS is higher than that of the two classical algorithms where the average localization errors of EWLS, LS, and PDM are 0.26702R, 0.29728R, and 0.28462R, respectively. This confirms that when WSNs exhibit the quasi-UDG connectivity behavior, our new hop-distance relationship that captures the behavior offers an improved accuracy in localization.

In the following, we further compare the localization accuracy among EWLS, LS and PDM under various scenarios. In these simulation experiments, we set N = 400, and sensor nodes are deployed uniformly in the circle area with the radius R_b = 200. The connectivity of nodes follows the quasi-UDG model. The localization error is calculated as $\xi = \sum_j \| \mathbf{x}_j - \hat{\mathbf{x}}_j \| / (N - n)$.

Firstly, we focus on the impact of the number of anchor nodes. The factor α of quasi-UDG model is set to 0.76 and the communication range R of each sensor node is set to 50. In Figure 8, we can see that the localization error ξ of all three algorithms decreases with the increase of number of anchor nodes. Among them, our proposed EWLS always offers the best performance.

Secondly, we investigate the impact of the parameter α of quasi-UDG model. In this scenario, we set the number of anchor nodes to 40 and the parameter α varies from 0.72 to 1. The localization error comparison is given in Figure 9. We observe that when the parameter α increases, the number of neighbor nodes increases

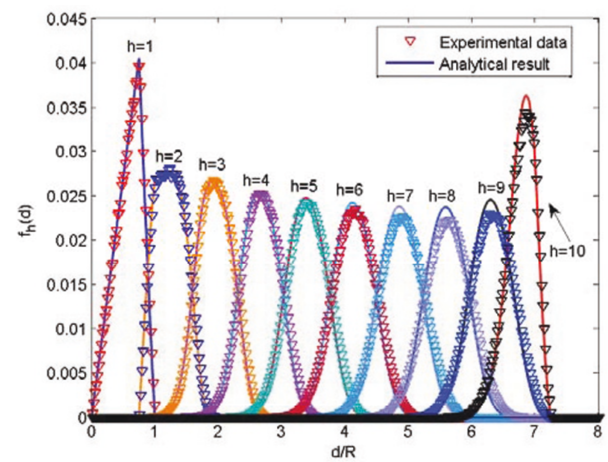

Figure 5 The distribution $f_{\mathcal{H}_{\mathcal{A}_1}}(d)$.

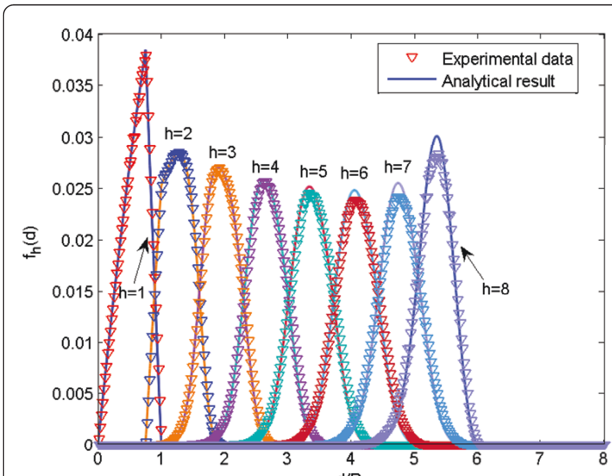

Figure 4 The distribution $f_{\mathcal{H}_{\mathcal{C}}}(d)$ when the hop count falls between 1 and 8.

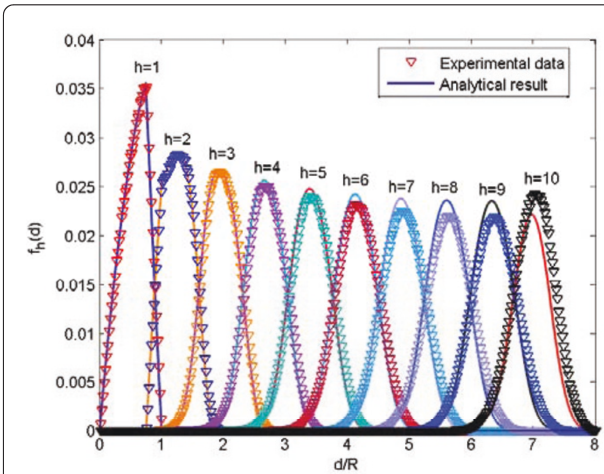

Figure 6 The distribution $f_{\mathcal{H}_{\mathcal{A}_2}}(d)$.

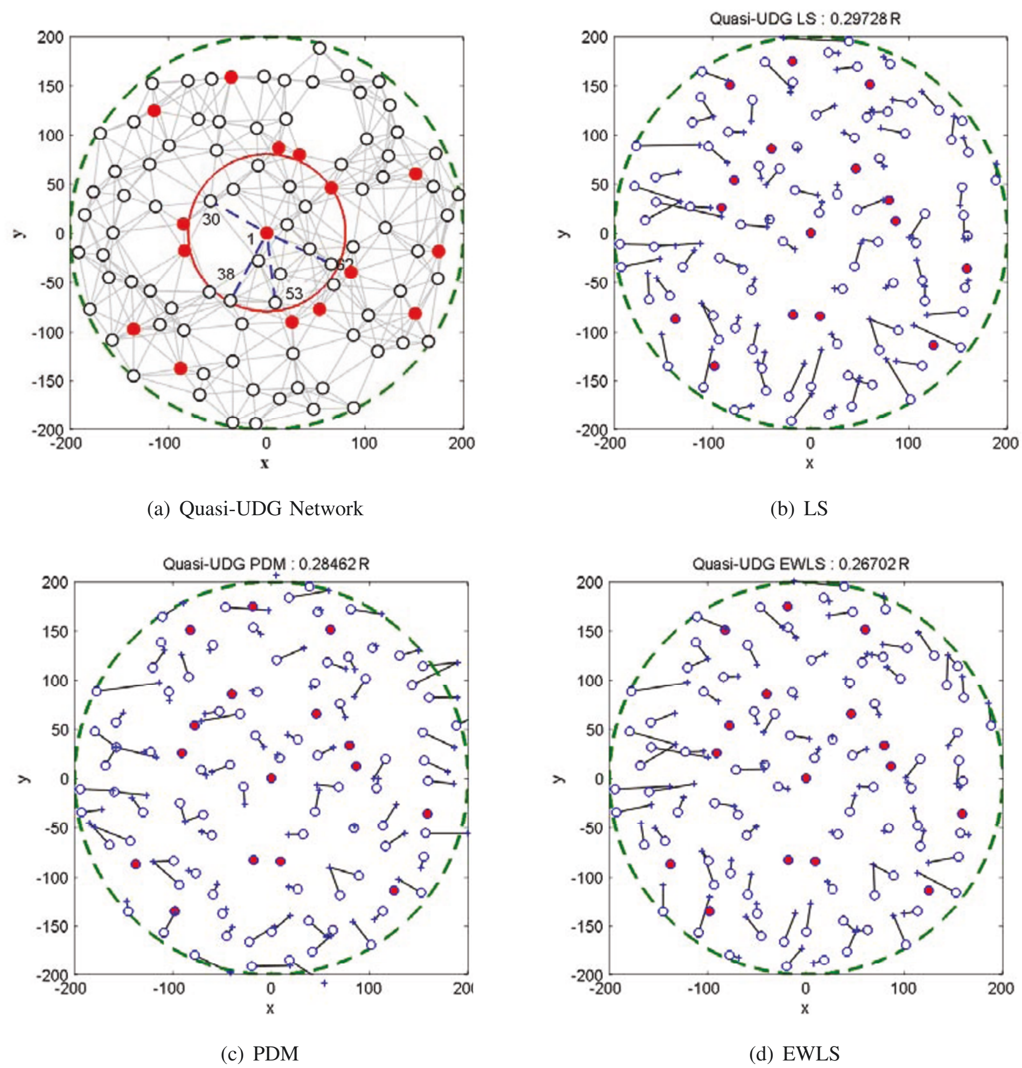

Figure 7 Localization error distributions on the quasi-UDG network topology.

and the number of hops between an unknown node and an anchor node decreases. Thus, the localization error decreases, and our proposed EWLS algorithm remains the best among all for all considered α values.

Last we study the impact of the communication range R of each sensor node. We set the parameter α of quasi-UDG model to 0.76 and set the number of anchor nodes to 40. Similarly, we compare the localization errors in Figure 10 with a range of R values. We observe that because the number of neighbor nodes of a node increases when its communication range increases, and number of hops between an unknown node and an anchor decreases which leads to a decrease in localization errors. Comparing the results for all algorithms, our proposed EWLS outperforms its peers.

7 Conclusions

The hop-distance relationship information can effectively improve the performance of the protocols for wireless sensor networks in many aspects. However, most studies focus on the UDG model which significantly deviates from the real world. In the paper, we presented an analytical modeling to formulate the hop-distance relationship considering the quasi-UDG model. Senor nodes are randomly distributed in a circular region according to a Poisson point process. The probability of a particular hop count given a known distance $\Omega_h(d)$ was studied, and the border effect and dependence problem was considered in our analysis. Precisely, we derived the probability density function of a random variable describing the distance between two arbitrary nodes with a given hop count.

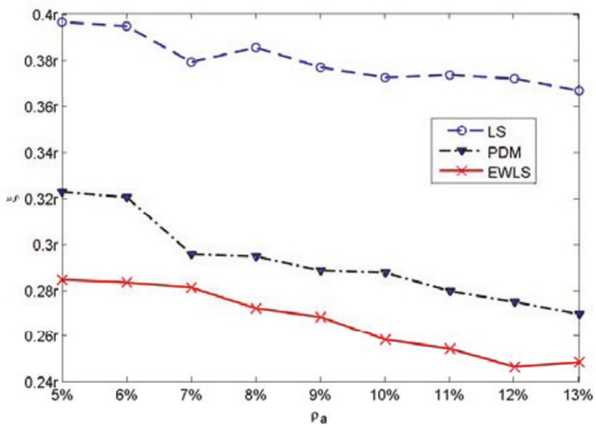

Figure 8 Effect on the average localization error ξ of anchor fraction ρ_a.

Simulation results confirmed that our analytical results gave excellent accuracy. From the results, we further illustrated impact of the border effect.

Furthermore, we demonstrated the application of our developed hop-distance relationship considering the quasi-UDG model in WSN localizations. We designed a LS-based localization algorithm using our developed relationship and compared its performance with other popular LS-based localization algorithms. We again confirmed that the explicit use of our developed relationship in the computation of localization algorithms improved the localization accuracy.

A Appendix

Suppose that a node $\mathbf{x}(x, y)$ is randomly deployed in a circular region with the radius R_b, the joint distribution $f_{\mathbf{x}}(x, y)$ can be obtained from

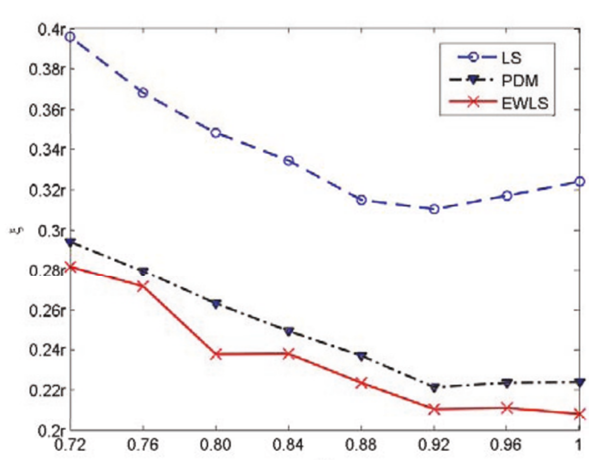

Figure 9 Effect on the average localization error of quasi-UDG factor α.

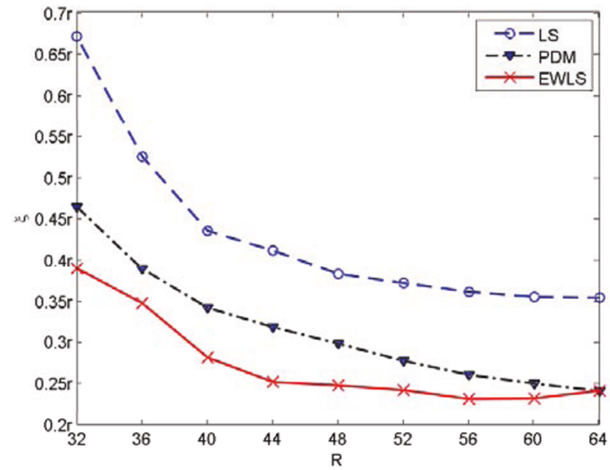

Figure 10 Effect on the average localization error ξ of nodes' communication range R.

$$f_{\mathbf{x}}(x, y) = \begin{cases} \frac{1}{\pi R_b^2}, & x^2 + y^2 \le R_b^2 \\ 0, & \text{elsewhere} \end{cases}. \tag{25}$$

As the nodes $\mathbf{x_1}(x_1, y_1)$ and $\mathbf{x_2}(x_2, y_2)$ are selected independently, the joint pdf of $\mathbf{x_1}$ and $\mathbf{x_2}$ is

$$f_{\mathbf{x_1},\mathbf{x_2}}(x_1, y_1, x_2, y_2) = \begin{cases} \frac{1}{(\pi R_b^2)^2}, & x_i^2 + y_i^2 \le R_b^2, \ i = 1, 2 \\ 0, & \text{e1sewhere} \end{cases} \tag{26}$$

We set $\mathbf{x_d} = \mathbf{x_1} - \mathbf{x_2}$ and $\mathbf{x_m} = (\mathbf{x_1} + \mathbf{x_2})/2$. The joint distribution of $\mathbf{x_m}$ and $\mathbf{x_d}$ can be obtained as

$$f_{\mathbf{x_d},\mathbf{x_m}}(x_d, \ y_d, x_m, \ y_m) = \begin{cases} \frac{1}{(\pi R_b^2)^2} & \mathbf{x_d}, \mathbf{x_m} \in L_1 \cap L_2 \\ 0, & \text{elsewhere} \end{cases} \tag{27}$$

where the constraints L_1 and L_2 are

$$\begin{aligned} L_1 &: (x_m + x_d/2)^2 + (y_m + y_d/2)^2 < R_b^2 \\ L_2 &: (x_m - x_d/2)^2 + (y_m - y_d/2)^2 < R_b^2. \end{aligned} \tag{28}$$

We set the probability of the geographical distance $\mathcal{D}$ between $\mathbf{x_1}$ and $\mathbf{x_2}$ less than d to be $P(\mathcal{D} \le d)$, and the constraint L_3 can be expressed by $L_3 : \mathcal{D}^2 = x_d^2 + y_d^2 \le d^2$, then we have

$$P(\mathcal{D} \le d) \iiiint\limits_{L_1 \cap L_2 \cap L_3} f_{\mathbf{x_d},\mathbf{x_m}}(x_d, y_d, x_m, y_m) \mathrm{d}x_m \mathrm{d}y_m \mathrm{d}x_d \mathrm{d}y_d. \tag{29}$$

With $L_1 \cap L_2$, then $\mathbf{x_m}$ falls into the intersectional region of two circles with centers $(x_d/2, y_d/2)$ and $(-x_d/2, -y_d/2)$. The intersectional area is

$$2R_b^2 \arccos\left(\frac{\sqrt{x_d^2 + y_d^2}}{2R_b}\right) - \sqrt{x_d^2 + y_d^2} \times \sqrt{R_b^2 - \left(\frac{x_d^2 + y_d^2}{4}\right)}. \tag{30}$$

Since $f_{\mathbf{x}_d,\mathbf{x}_m}(x_d, y_d, x_m, y_m)$ is constant, (29) can be rewritten as

$$P(\mathcal{D} \le d) = \frac{1}{\pi R^4} \int_0^d \left[4R^2 \arccos\left(\frac{l}{2R}\right) - l\sqrt{4R^2 - l^2} \right] l \mathrm{d}l \quad (31)$$

Therefore, we have

$$f_{\mathcal{D}}(d) = \frac{d}{\pi R^4} \left(4R^2 \arccos\left(\frac{d}{2R}\right) - d\sqrt{4R^2 - d^2} \right) \quad (32)$$

where $0 < d < 2R_b$.

Acknowledgements
The authors gratefully acknowledge the support of the Program of Introducing Talents of Discipline to Universities ("111 Project") under grant No. B08002, and the support of the National Natural Science Foundation of China (NSFC) under Grants No. 60802016, 60833002 and 60972010, the support by "the Fundamental Research Funds for the Central Universities" under grant No. 2009JBM007.

Author details
[1]School of Electronics and Information Engineering, Beijing Jiaotong University, Beijing 100044, PR China [2]TEDA College, Nankai University, Tianjin 300457, PR China [3]School of Computer Engineering, Nanyang Technological University, 639798, Singapore

Competing interests
The authors declare that they have no competing interests.

Received: 31 December 2010 Accepted: 17 September 2011
Published: 17 September 2011

References

1. DG Jennifer Yick, M Biswanath, Wireless sensor network survey. Comp Netw. **52**, 2292–2330 (2008). doi:10.1016/j.comnet.2008.04.002
2. D Niculescu, Positioning in ad hoc sensor networks. IEEE Netw. **18**(4), 24–29 (2004). doi:10.1109/MNET.2004.1316758
3. N Patwari, JN Ash, S Kyperountas, AO Hero, RL Moses, NS Correal, Locating the nodes: cooperative localization in wireless sensor networks. IEEE Signal Process Mag. **22**(4), 54–69 (2005)
4. H Breu, DG Kirkpatrick, Unit Disk Graph Recognition is NP-hard. Computational Geometry. **9**(1-2), 3–24 (1998). doi:10.1016/S0925-7721(97)00014-X
5. F Kuhn, T Moscibroda, R Wattenhofer, Unit disk graph approximation, in *Proc. Joint Workshop on Foundations of Mobile Computing, Philadelphia, PA, USA*, 17–23 (October 2004)
6. D Niculescu, B Nath, DV based positioning in ad hoc networks. Telecommun Syst. **22**(14), 267–280 (2003)
7. T He, C Huang, BM Blum, JA Stankovic, T Abdelzaher, Range-free localization schemes for large scale sensor networks, in *Proc International Conference on Mobile Computing and Networking (MobiCom)*, California 81–95 (September 2003)
8. J-P Sheu, P-C Chen, C-S Hsu, A distributed localization scheme for wireless sensor networks with improved grid-scan and vector-based refinement. IEEE Trans Mobile Comput. **7**(9), 1110–1123 (2008)
9. Y Shang, W Ruml, Y Zhang, M Fromherz, Localization from connectivity in sensor networks. IEEE Trans Parallel Distribu Syst. **15**(11), 961–974 (2004). doi:10.1109/TPDS.2004.67
10. PD Tinh, M Kawai, Distributed range-free localization algorithm based on self-organizing maps. EURASIP J Wireless Commun Netw. **2010** (2010)
11. S Dulman, M Rossi, P Havinga, M Zorzi, On the hop count statistics for randomly deployed wireless sensor networks. Int J Sensor Netw. **1**(1/2), 89–102 (2006). doi:10.1504/IJSNET.2006.010837
12. R Flury, SV Pemmaraju, R Wattenhofer, ZE Zurich, Greedy routing with bounded stretch, in *Proc IEEE International Conference on Computer Communications (INFOCOM)*, Rio de Janeiro, Brazil 1737–1745 (April 2009)
13. S Ruhrup, H Kalosha, A Nayak, I Stojmenovic, Message-efficient beaconless georouting with guaranteed delivery in wireless sensor, ad hoc, and actuator networks. IEEE/ACM Trans Netw. **18**(1), 95–108 (2010)
14. Z Zhou, Z Peng, J-H Cui, Z Shi, A Bagtzoglou, Scalable localization with mobility prediction for underwater sensor networks. IEEE Trans Mobile Comput. **10**(3), 335–348 (2011)
15. M Kadivar, ME Shiri, M Dehghan, Distributed topology control algorithm based on one- and two-hop neighbors' information for ad hoc networks. Computer Communications. **32**(2), 368–375 (2009). doi:10.1016/j.comcom.2008.11.014
16. F Khadar, D Simplot-Ryl, Incremental power topology control protocol for wireless sensor networks, in *Proc IEEE International Symposium on Personal, Indoor and Mobile Radio Communicatoins (PIMRC)*, Tokyo, Japan, 77–81 (September 2009)
17. SAG Chandler, Calculation of number of relay hops required in randomly located radio network. Electronics Letters. **25**(24), 1669–1671 (1989). doi:10.1049/el:19891119
18. C Bettstetter, J Eberspacher, Hop distances in homogeneous ad hoc networks, in *Proc IEEE Vehicular Technology Conference (VTC 2003-Spring)*, Jeju Island, Korea 2286–2290 (April 2003)
19. Z Li, W Trappe, Y Zhang, B Nath, Robust statistical methods for securing wireless localization in sensor networks, in *Proc International Symposium on Information Processing in Sensor Networks (IPSN)*, California, 91–98 (April 2005)
20. E Ekici, J Mcnair, D Al-Abri, A probabilistic approach to location verification in wireless sensor networks, in *Proc IEEE International Conference on Communications (ICC)*. **8**, 3485–3490 (2006)
21. L Zhao, Q Liang, Hop-distance estimation in wireless sensor networks with applications to resources allocation. EURASIP J Wireless Commun Netw. **2007** (2007)
22. X Ta, G Mao, BDO Anderson, Evaluation of the probability of k-hop connection in homogeneous wireless sensor networks, in *Proc Global Telecommuniations Conference (GLOBECOM)*, Washington, 1279–1284 (November 2007)
23. D Ma, MJ Er, B Wang, HB Lim, K-hop statistics in wireless sensor networks, in *Proc International Conference on Intelligent Sensors, Sensor Networks and Information Processing (ISSNIP)*, Melbourne, Austrilia, 469–474 (December 2009)
24. J Chen, A Jiang, IA Kanj, G Xia, F Zhang, Separability and topology control of quasi unit disk graphs, in *Proc IEEE International Conference on Computer Communications (INFOCOM)*, Alaska, 2225–2233 (May 2007)
25. C Bettstetter, On the minimum node degree and connectivity of a wireless multihop network, in *Proc International Symposium on Mobile Ad Hoc Networking and Computing (MobiHoc)*, Lausanne, Switzerland, 80–91 (June 2002)
26. A Savvides, C-C Han, MB Strivastava, Dynamic fine-grained localization in ad-hoc networks of sensors, in *Proc International Conference on Mobile Computing and Networking (MobiCom)*, Rome, Italy 166–179 (July 2001)
27. H Lim, JC Hou, Localization for anisotropic sensor networks, in *Proc IEEE International Conference on Computer Communications (INFOCOM)*, Miami 138–149 (March 2005)

doi:10.1186/1687-1499-2011-99
Cite this article as: Gao *et al.*: **Hop-distance relationship analysis with quasi-UDG model for node localization in wireless sensor networks.** *EURASIP Journal on Wireless Communications and Networking* 2011 **2011**:99.